June 01, 1976

Three-dimensional nonlinear numerical analysis of solid-rotor induction motor

Mulukutla S. Sarma
Northeastern University

THREE-DIMENSIONAL NONLINEAR NUMERICAL ANALYSIS OF SOLID-ROTOR INDUCTION MOTOR

Dr. Mulukutla S. Sarma
Department of Electrical Engineering
Northeastern University
Boston, Mass. 02115, U.S.A.

1. Summary

The most elementary type of rotor for the polyphase induction machine is the solid-iron rotor, which offers advantages in ease of manufacture, in high torque per ampere at standstill, in withstanding high rotational stresses, and in operating in unusual environments. Since conventional induction machine theory has proven inadequate for such machines, the need has arisen for improved methods of investigation. It is the purpose of this paper to present an approximate three-dimensional nonlinear numerical analysis for the solid-rotor induction motor, based on magnetostatic assumptions and finite-difference iterative techniques.

2. Introduction

The interaction between the eddy currents induced in the solid cylindrical rotor steel structure and the revolving field of the airgap produces the electrodynamic torque. Recently there has been wide interest in the possible use of such solid-rotor motors for ultra high-speed inverter drives with suitable high stator supply frequency as well as variable speed drives for conventional frequencies and speed ranges. Also the solid-rotor machine has characteristics that are particularly suitable for solid-state power controls. Very efficient, small, light-weight electrical power equipment is in demand due to operational and military requirements.

The difficult problems of analyzing the solid-rotor induction motors and developing lumped-parameter equivalent circuits wherever possible has occupied designers and research workers for many years. Conventional induction machine theory has proven inadequate for such machines, and the need has arisen for improved methods of investigation. A number of analytical methods of analysis for the solid-rotor induction motors have been developed in the recent years: (McConnell and Sverdrup (1955), Wood and Concordia (1960), Finzi and Paice (1968), Heller and Sarma (1968), Wilson (1969), Sarma and Soni (1972).

Also, numerical methods of analysis have been explored: (Wilson, Hopkins, and Erdelyi (1965), Sarma and Erdelyi (1969), Wilson (1969). The nonlinear two-dimensional electromagnetic field analysis of the solid-rotor induction machine has been attempted (Wilson, 1969) and a sophisticated digital computer program has been developed with considerable ingenuity, while taking into account the field-dependent rotor magnetic permeability. An approximate 3-dimensional nonlinear numerical analysis will now be presented in this paper for the solid-rotor induction motor.

3. Assumptions And Mathematical Model

3.1 Assumptions Made

The solution will be based on magnetostatic assumptions. Only one pole pitch is considered in the analysis, as the solution is periodic in the peripheral direction. The curvature of the rotor and stator will not be considered, so that a Cartesian coordinate system can be used. The permeability of the stator stampings is assumed to be infinite. The stator currents are replaced by a surface current sheet so as to match approximately the constant voltage operation of the motor. The air gap of the model is assumed to be zero as it will be easy to correct later for this assumption when computing the performance characteristics of the motor. The effect of the stator end windings as well as the end regions will not be considered, and the analysis is terminated at the end of the rotor surface in the axial direction.

Only one part of the rotor half will be investigated. In order to use less computer storage and time, the solution of the two-dimensional nonlinear problems will be assumed at a fixed boundary located at a convenient distance from the rotor end. At a certain rotor depth, all the vector potentials will be set according to the two-dimensional linear solution and be treated as fixed. This rotor depth in the radial direction is chosen for each value of slip in accordance with the results of the two-dimensional solutions. As a first approximation, it will be assumed that the axial component of the flux density, B_z, is zero everywhere in the entire region. The justification for this step stems from the analysis of three-dimensional linear solution, and from the fact that the axial component of the flux density is indeed small and exists only in a small portion of the end of the rotor. It can be shown that the problem can be posed in terms of the axial component of the vector potential, A_z, when it is assumed that B_z is equal to zero. Hence, only A_z exists in the entire region. The radial and the tangential components of the vector potential, A_x and A_y, are set equal to zero in the entire region.

All materials are taken to be isotropic and homogeneous. The conductivity of the rotor material is taken to be a constant. The permeability of the ferromagnetic materials, μ, is taken to be a single valued function of the magnetic induction, $\bar{B}$. Piecewise linear representation of the magnetization curve for computer use has been done as in Trutt, Erdelyi, and Hopkins (1965). The dielectric effects are neglected. Rationalized MKSA system of units has been used throughout, unless otherwise specified.

3.2 Coordinate System

Referring to Figure 1, one plane of the coordinate system is taken along the axis of the solid rotor induction motor. The bore periphery represents the y-axis and x-axis is radial. The coordinate system is fixed with respect to the rotating field, and its origin

is conveniently located at a point '0', as shown in Figure 1. The partial differential equations will be first developed in terms of general space coordinates x, y, z, and time t, fixed to the medium under consideration. They will then be transformed to a system fixed with respect to the rotating field.

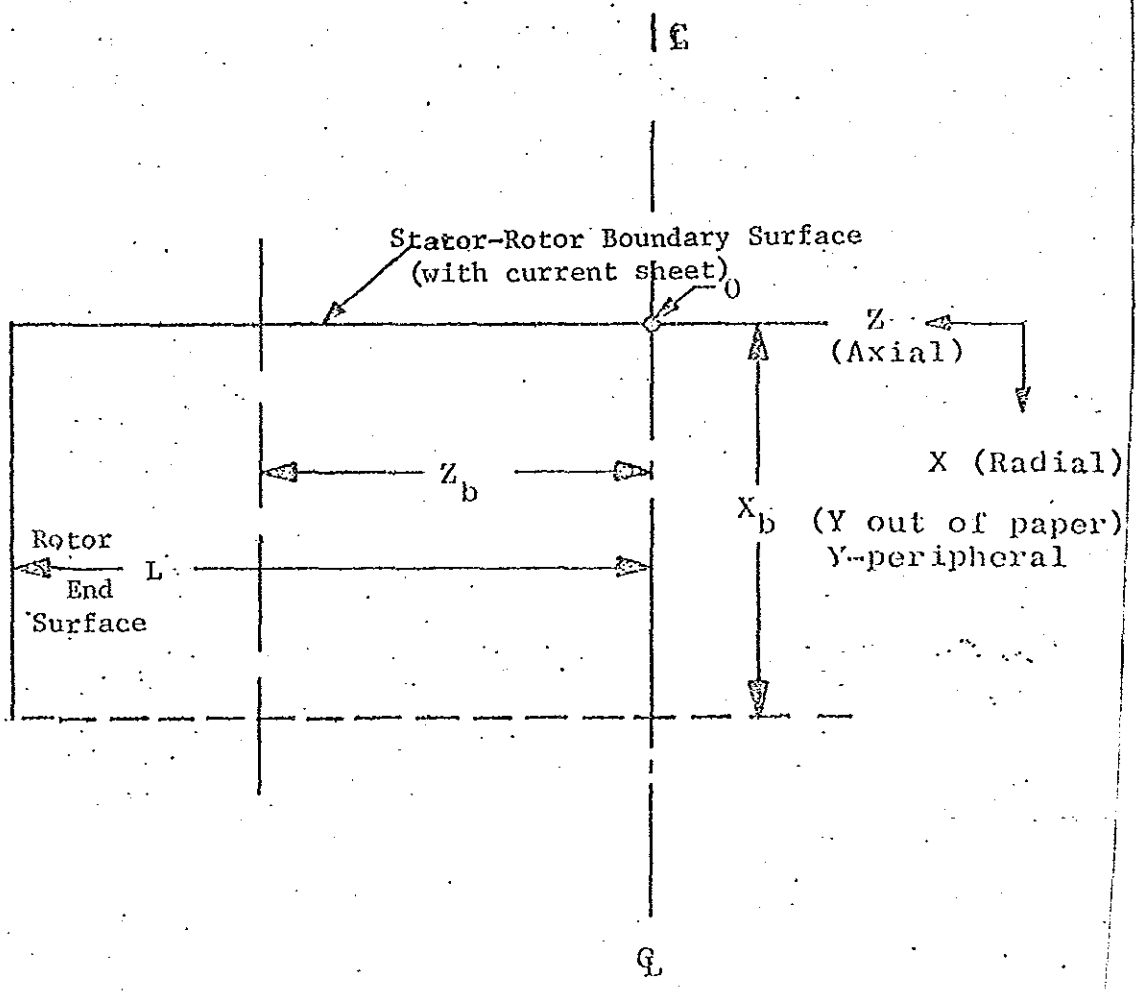

Figure 1: Mathematical Model of the Solid Rotor Induction Motor

4. Three-Dimensional Field Equations

4.1 Three-Dimensional Nonlinear Vector Field Equations in Cartesian Coordinates

For material regions which are void of electric charge and impressed current densities, but in which conduction current densities exist due to induction phenomena, the relevant Maxwell's equations in differential form are given below:

$$\nabla \times \bar{H} = \bar{J} \; ; \; \nabla \cdot \bar{B} = 0 \; ; \; \nabla \times \bar{E} = - \frac{\partial \bar{B}}{\partial t} \qquad (1,2,3)$$

The constituent relations are given by

$$\bar{B} = \mu \bar{H} \; ; \; \bar{J} = \sigma \bar{E} \qquad (4,5)$$

where μ is the permeability and σ the conductivity. In terms of a magnetic vector potential, one can write

$$\bar{B} = \nabla \times \bar{A} \; ; \; \bar{E} = - \frac{\partial \bar{A}}{\partial t} - \nabla \phi \qquad (6,7)$$

where ϕ is an electric scalar potential. Defining the reluctivity, ν, as the reciprocal of the magnetic permeability, μ, one can obtain

$$\nabla \times [\nu (\nabla \times \bar{A})] = -\sigma [\frac{\partial \bar{A}}{\partial t} + \nabla \phi] \qquad (8)$$

The scalar potential ϕ has to satisfy the following equation:

$$\nabla^2 \phi = - \frac{\partial}{\partial t} (\nabla \cdot \bar{A}) \qquad (9)$$

which is a consequence of Eq. (8). With the assumption that the vector potential has only one component, A_z, the subscript z of A_z may now be dropped, so that

$$\bar{A} = \bar{a}_z A_z = \bar{a}_z A \qquad (10)$$

Eq. (8) yields coupled component partial-differential equations. Uncoupling is achieved through appropriate arbitrary definitions of divergence of $\bar{A}$ and the gradient of ϕ. By defining that

$$- \sigma \frac{\partial \phi}{\partial x} = \frac{\partial}{\partial z} (\nu \frac{\partial A}{\partial x}) \; ; \; - \sigma \frac{\partial \phi}{\partial y} = \frac{\partial}{\partial z} (\nu \frac{\partial A}{\partial y}) \; ; \; - \sigma \frac{\partial \phi}{\partial z} = \frac{\partial}{\partial z} (\nu \frac{\partial A}{\partial z}) \qquad (11,12,13)$$

the following partial-differential equation can be obtained for the description of the fields:

$$\frac{\partial}{\partial x} (\nu \frac{\partial A}{\partial x}) + \frac{\partial}{\partial y} (\nu \frac{\partial A}{\partial y}) + \frac{\partial}{\partial z} (\nu \frac{\partial A}{\partial z}) = \sigma \frac{\partial A}{\partial t} \qquad (14)$$

The components of the flux density and of the electric field intensity may simply be evaluated in terms of A as follows:

$$B_x = \frac{\partial A}{\partial y} \; ; \; B_y = - \frac{\partial A}{\partial x} \; ; \; B_z = 0 \qquad (15,16,17)$$

$$E_x = \frac{1}{\sigma} \frac{\partial}{\partial z} (\nu \frac{\partial A}{\partial x}) \; ; \; E_y = \frac{1}{\sigma} \frac{\partial}{\partial z} (\nu \frac{\partial A}{\partial y}) \; ; \; E_z = - \frac{\partial A}{\partial t} + \frac{1}{\sigma} \frac{\partial}{\partial z} (\nu \frac{\partial A}{\partial z}) \qquad (18,19,20)$$

So far, the equations have been developed in terms of a coordinate system fixed to either the stator or the rotor. In order to eliminate the time coordinate in the equations, a coordinate transformation will be performed, so that the new coordinate system will be

stationary with respect to the rotating field. The following transformation equations are used:

$$x = x_s = x_r \; ; \; z = z_s = z_r \; ; \; y = \frac{\pi}{\tau} y_s - \omega t_s = \frac{\pi}{\tau} y_r - S\omega t_r \qquad (21,22,23)$$

where S is the per-unit slip; ω is stator supply angular frequency ; τ is the pole pitch; and subscripts s and r refer to stator and rotor respectively. The partial-differential equations are then transformed to the following:
In the airgap:

$$\frac{\partial^2 A(a)}{\partial x^2} + \frac{\pi^2}{\tau^2} \frac{\partial^2 A(a)}{\partial y^2} + \frac{\partial^2 A(a)}{\partial z^2} = 0 \qquad (24)$$

In the linear region of the rotor:

$$\frac{\partial^2 A(r)}{\partial x^2} + \frac{\pi^2}{\tau^2} \frac{\partial^2 A(r)}{\partial y^2} + \frac{\partial^2 A(r)}{\partial z^2} + S\omega\mu_\ell \sigma \frac{\partial A(r)}{\partial y} = 0 \qquad (25)$$

In the nonlinear region of the rotor:

$$\frac{\partial}{\partial x}\left(\nu \frac{\partial A(r)}{\partial x}\right) + \frac{\pi^2}{\tau^2} \frac{\partial}{\partial y}\left(\nu \frac{\partial A(r)}{\partial y}\right) + \frac{\partial}{\partial z}\left(\nu \frac{\partial A(r)}{\partial z}\right) = -S\omega\sigma \frac{\partial A(r)}{\partial y} \qquad (26)$$

The field components, in the interior of the rotor, will transform as follows:

$$B_x = \frac{\pi}{\tau} \frac{\partial A}{\partial y} \; ; \; B_y = -\frac{\partial A}{\partial x} \; ; \; B_z = 0 \qquad (27,28,29)$$

$$E_x = \frac{1}{\sigma} \frac{\partial}{\partial z}\left(\nu \frac{\partial A}{\partial x}\right) \; ; \; E_y = \frac{1}{\sigma} \frac{\pi}{\tau} \frac{\partial}{\partial z}\left(\nu \frac{\partial A}{\partial y}\right) \; ; \; E_z = S\omega \frac{\partial A}{\partial y} + \frac{1}{\sigma} \frac{\partial}{\partial z}\left(\nu \frac{\partial A}{\partial z}\right) \qquad (30,31,32)$$

4.2 Transformation of Partial Differential Equations to Difference Equations

The partial differential equations have to be transformed into the difference form for numerical work. The difference expressions can be developed either by directly using the partial-differential equations and the first two terms of Taylor series, or by applying Ampere's law. Figure 2 shows a typical three-dimensional lattice. The distance between the point 0 and the points 1-6 are denoted by h_1-h_6, respectively. Figure 3 shows a typical lattice point 0 and its neighborhood; points I-VI are located at the middle points of the mesh lines 01-06, respectively; ν_I-ν_{VI} are the reluctivities specified at the center points I-VI, respectively; J_0 is the current-density vector specified at the lattice point 0.

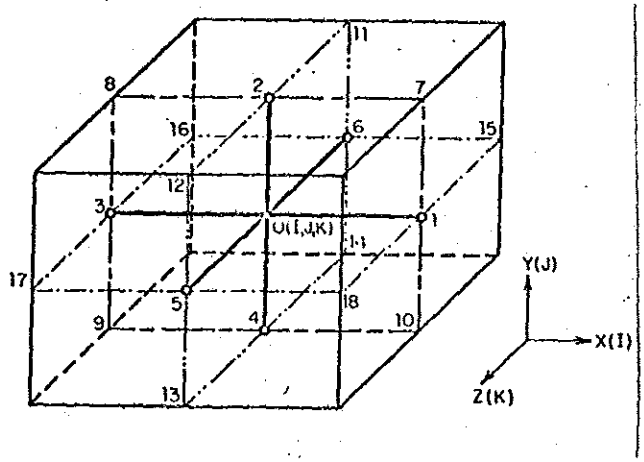

Figure 2: Typical Three-Dimensional Lattice

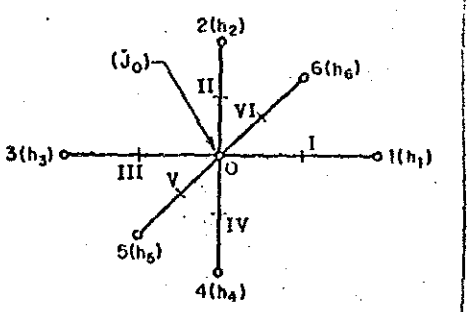

Figure 3: Typical Lattice Point and its Neighborhood

Eq. (26) yields the following difference expression for A_o in the rotor:

$$A_o = \frac{(S\omega\sigma A_2/h_2) + \sum_{i=1}^{6} \nu_i \alpha_i A_i}{(S\omega\sigma/h_2) + \sum_{i=1}^{6} \nu_i \alpha_i} \qquad (33)$$

The reluctivities may more naturally be specified at the centers of the parallelepipeds as being common to an elemental volume, and these may be easily related to those specified ealier at the center points of the lattice lines. The flux density at the center of each parallelepiped can be evaluated and the corresponding reluctivity can be computed from the magnetization curve.

5. Numerical Solution

A suitable fine lattice system is laid out on the mathematical model for numerical analysis. The number of lattice points and the region to be considered for sufficiently accurate results depend on the value of the slip. The boundary conditions are then specified in differential and difference forms, as discussed in detail by Sarma and Erdelyi (1969). The periodicity condition is to be satisfied in the peripheral y direction. The z-component of the current density must vanish at the rotor-end surface. The surface current sheet at the stator-rotor boundary surface is to be matched appropriately.

An iterative procedure is then developed for the numerical solution of the nonlinear partial differential equations. In each iteration, the vector potentials at each of the lattice points are calculated, using reluctivities calculated during the previous iteration, by successive point relaxation method; later the reluctivities are recomputed using the newly calculated vector potentials and are

underrelaxed. A new method of computing an appropriate relaxation factor for the reluctivity at each lattice point depending on its location on the magnetization characteristic has been successfully implemented. This method has resulted in some significant improvement in convergence. The details of this method are given by Sarma and Erdelyi (1969) and Wilson (1969), and cannot be presented here in view of the space limitations. The adopted iterative scheme carries out the computations plane by plane (xy planes) along the positive z direction. Sweeping has been done in the positive y direction on a given line in the xy plane, then in the positive x direction, and then in the positive z direction on all the xy planes, thereby covering all the lattice points in the model.

The convergence is judged by the fact that the algebraic sum of the residuals and the sum of the absolute values of residuals of the vector potential are monotonic functions and the sum is of the order of the average value of the vector potentials. Thereby, the average residual is of the order of less than 0.01 per cent of the average vector potential. The number of iterations required for an acceptable convergence is of the order of 100 iterations for about 20,000 lattice points.

6. Terminal Characteristics

In order to find the terminal voltage, the voltage induced in the armature winding by the resultant flux distribution in the airgap will be found first. The impedance drops in the stator can then be added to find terminal voltage. The specification of the current sheet on the stator-rotor boundary surface in the analysis can be changed by trial until one does get the desired voltage.

The torque of the solid rotor is calculated from the well-known relationship between the mechanical output and the ohmic losses in the rotor:

$$P_{mech} = P_{\Omega} \frac{1-S}{S} \tag{34}$$

The torque is then found as

$$T = \frac{P_{mech}}{\omega_m} = P_{\Omega} \frac{1-S}{S} \frac{p}{\omega_S(1-S)} = \frac{P_{\Omega} p}{S\omega_S} \tag{35}$$

where p is the pairs of poles. The ohmic losses are easily evaluated from the volume integral of the squared current densities.

The computer program is so developed that it can easily be modified for other values of slip. The dimensions X_b and Z_b of Figure 1 need to be decided judiciously and a new convenient lattice system is to be chosen. After satisfactory convergence, the current densities and flux densities at all the lattice points, as well as the torque and the terminal voltage are evaluated. The computed results indicate the following characteristics:

The end region of the solid rotor of the induction motor is more and more saturated as the end surface is approached. The nonlinear portion increases continuously. The nonlinear depth at the end surface of the rotor is about twice that at the center of the rotor. The x and y components of the current densities become significant only in the last 1/20th part of the rotor. The z component of the current density is significant throughout, although it is zero right on the end surface of the rotor. The radial flux density shows a significant rise in the end part of the rotor.

The numerical method has been established here for finding the three-dimensional current density distribution in the solid rotor of high-speed induction motors, in order to calculate the performance characteristics. It is only a first approximation, and further refinements are suggested by Sarma and Erdelyi (1969). The presented method has been applied to analyze a 5-HP, 6-pole, 3200-Hz, three-phase, 145-volts, star-connected solid-rotor induction machine.

7. Acknowledgements

The author likes to express his sincere thanks to Professor E.A. Erdelyi, Dr. J.C. Wilson, and Dr. A.L. Jokl for their helpful suggestions and discussions. The presented analysis is a part of the outcome of the contract No. DA-44-009-AMC-787(T) given to the University of Colorado by the U.S. Army Mobility Equipment Research and Development Center, Fort Belvoir, Va.

8. References

FINZI, L.A., and PAICE, D.A. (1968): "Analysis of the solid iron rotor induction motor for solid-state speed controls", IEEE Trans. Power Apparatus and Systems, Vol. PAS-87, p.590.

HELLER, B., and SARMA, M.S. (1968): "The electromagnetic field in solid iron", Acta Tech. (Prague), No. 6.

McCONNELL, H.M., and SVERDUP, E.F. (1955): "The induction machine with solid iron rotor", AIEE Trans. Power Apparatus and Systems, Vol. 74, p. 343.

SARMA, M.S., and ERDELYI, E.A. (1969): "Synthesis of high speed homopolar alternators and theory of solid rotor electrical machines, phase DD, pt. IV", USAMERDC Report, Fort Belvoir, Va.

SARMA, M.S., and SONI, G.R. (1972): "Solid-rotor and composite-rotor induction machines", IEEE Trans. Aerospace and Electronic Systems, Vol. AES-8, No. 2, p. 147.

TRUTT, F.C., ERDELYI, E.A., and HOPKINS, R.E. (1968): "Representation of the magnetization curve of D.C. machines for computer use", IEEE Trans. Power Apparatus and Systems, Vol. PAS-87, No. 3

WILSON, J.C., ERDELYI, E.A., and HOPKINS, R.E. (1965): "Aerospace composite-rotor induction motors", supplement to IEEE Trans. Aerospace, Vol. AES-3.

WILSON, J.C. (1969): "Theory of the solid-rotor induction machine", Ph.D. Dissertation, University of Colorado, Boulder, Colo.

WOOD, A.J., and CONCORDIA, C. (1960): "An analysis of solid-rotor machines, Pt. 111: Finite length effects, Pt. IV: An approximate nonlinear analysis", AIEE Trans. Power Apparatus and Systems, vol. 79.

9. Appendix

The α_i's of Eq. (33) are given below:

$$\alpha_1 = \frac{2}{h_1(h_1 + h_3)} \quad ; \alpha_3 = \frac{2}{h_3(h_1 + h_3)}$$

$$\alpha_2 = \frac{2}{h_2(h_2 + h_4)} \frac{\pi^2}{\tau^2} \quad ; \alpha_4 = \frac{\pi^2}{\tau^2} \frac{2}{h_4(h_2 + h_4)}$$

$$\alpha_5 = \frac{2}{h_5(h_5 + h_6)} \quad ; \alpha_6 = \frac{2}{h_6(h_5 + h_6)}$$